


Cite this: *RSC Adv.*, 2021, **11**, 26915

Received 23rd March 2021
Accepted 3rd August 2021

DOI: 10.1039/d1ra02298a
rsc.li/rsc-advances

Red, green, and blue light-emitting carbon dots prepared from *o*-phenylenediamine†

Yulong An, ^a Xu Lin, ^a Yuxi Zhou, ^a Yan Li, ^a Yunwu Zheng, ^b Chunhua Wu, ^b Kaimeng Xu, ^b Xijuan Chai^b and Can Liu^{*ab}

Carbon dots (CDs), as the most important type of carbon-based material, have been widely used in many fields because of their excellent properties. In particular, multicolor fluorescent CDs with high photoluminescence quantum yield are the focus of active research. Herein, red, green and blue CDs (RGB CDs) were successfully synthesized by a solvothermal method from *o*-phenylenediamine under different reaction conditions. The RGB-CDs have stable optical properties and significant photoluminescence characteristics. Structural and elemental analyses propose a conjugated structure and the surface state of the CDs as the main causes for the different color emission of RGB-CDs. In addition, a white fluorescent CD solution was prepared by mixing these multicolor fluorescent CDs in appropriate proportions.

Introduction

Since the discovery of Carbon Dots (CDs) in 2004, great progress has been made in their applications including in solar cells, photocatalysis, sensing detection, and biomedical applications.^{1,2} Recently, to construct intelligent photovoltaic systems, there has been an increasing demand for improving the functional characteristics of CDs in photovoltaic devices.³ For instance, applying CDs in optoelectronic devices results in tunable PL emissions, modified surface structure, chemical doping, and solid-liquid PL.^{4,5} To obtain superior CDs, efforts should be devoted to the design and synthesis of multicolour fluorescent CDs.

Trichromatic luminescence and high PLQYs are essential to realize full-color display. The CDs with visible spectral emission can be obtained through a one pot pyrolysis method by adjusting the precursor or reaction conditions.^{6–10} Lin *et al.*¹¹ developed a variety of colored fluorescent CDs using different precursors, and differences in particle size and nitrogen content were proposed to result in red-shifted emission. The emission wavelength of CDs changed from 426 to 603 nm by changing the precursors from (*o*-, *m*-, *p*-) phenylenediamine, and tricolour CDs were prepared. Bai *et al.*¹² used citric acid and urea as precursors, and the luminescence of CDs changed from blue and green to red when the solvent was used water, ethanol, and dimethylformamide (DMF), respectively.

Detailed characterization has shown that the eigenstates and surface states associated with C=O/C=N are derived from the multistate absorptions and blue, green, and red emission of CDs. Xiong and Yang's team¹³ used 3,5-diaminobenzoic acid and 3,4-diaminobenzoic acid to obtain red, green, and blue (RGB) color-emitting CDs (RGB-CDs) *via* a one-pot solvothermal route. The conjugated graphite structure of the carbon cores and the presence of oxygen on the surface states were the main causes for the RGB color emissions of CDs. However, at present, there are still many problems, such as the synthesis method is relatively complex and the source of raw materials is limited. Therefore, developing simple methods to prepare polychromatic CDs is still a great challenge.

In this study, we report the preparation of multicolour luminescent CDs using a simple one-pot pyrolysis method. By using *o*-phenylenediamine as the reaction precursor, adding reaction auxiliaries, and changing the reaction conditions, red, green, and blue luminescent CDs were obtained. The low cost of the precursor is of great significance for further developing the electro-optical application and the batch synthesis of CDs. The three CDs showed excellent and stable PL performance in solutions. Furthermore, a stable white fluorescent CDs solution was prepared by mixing the three CD solutions in appropriate proportions.

Materials and methods

Materials

o-Phenylenediamines (99%), ethanol (99.7%), potassium hydrogen sulfate (99.0%) and methylene chloride (99%) were provided by Shanghai Titan Scientific Co., Ltd (Shanghai, China). All reagents were used as received without further purification unless otherwise specified. Deionized (DI) water was used throughout this study.

^aKey Laboratory for Forest Resources Conservation and Utilization in the Southwest Mountains of China, College of Material Science & Engineering, Southwest Forestry University, Kunming, China. E-mail: liucanswf@163.com

^bKey Laboratory of State Forestry Administration for Highly-Efficient Utilization of Forestry Biomass Resources in Southwest China, Southwest Forestry University, Kunming, China

† Electronic supplementary information (ESI) available. See DOI: 10.1039/d1ra02298a



Methods

Transmission electron microscopy (TEM) images was carried out using a FEI Tecnai G2 F20 operating at an acceleration voltage of 200 kV. UV-Vis spectra were recorded with a Shimadzu UV-2600 spectrometer. Fluorescence measurements were collected using a Shimadzu fluorescence spectrophotometer RF-6000. Nanosecond fluorescence lifetime experiments were performed by the time correlated single-photon counting (TCSPC) system (HORIBA Scientific iHR 320). A 290 nm (<1 ns) and a 485 nm (<200 ps) nano-LED light source were used to excite the samples. CIE chromaticity coordinate was measured by KONICA MINOLTA CS-150 colorimeter. The Fourier transform infrared (FT-IR) spectra were obtained in transmission mode on a Thermo Scientific Nicolet iS5 spectrometer (Waltham, MA, USA) with the KBr pellet technique, and 8 scans at a resolution of 1 cm^{-1} were accumulated to obtain one spectrum. X-ray photoelectron spectroscopy (XPS) was investigated by using K-Alpha spectrometer with a mono X-ray source Al $\text{K}\alpha$ excitation (1486.6 eV). Binding energy calibration was based on C 1s at 284.8 eV.

Quantum yield measurements

Absolute PLQY measurements were performed in a FLS1000 spectrometer equipped with a calibrated integrating sphere. We conducted the test light from a FLS1000 spectrometer to the sphere. The PLQY was determined by the ratio between photons emitted and absorbed by CDs. The aqueous solution of CDs was placed in a cuvette to measure its QY, while the solvent water was used as a blank sample for the reference measurement.

Synthesis of R-CDs, G-CDs and B-CDs

o-Phenylenediamine (0.5 g or 2.0 g) was dissolved in 10 mL ethanol, and then the solutions was transferred into poly(tetrafluoroethylene)-lined autoclaves. After heating at 180 °C or 230 °C in oven for 12 h and cooling down to room temperature naturally, green and blue fluorescent suspensions were obtained from carbonized at different concentration and temperatures, respectively. In addition, potassium bisulfate (0.1 g) mixed with *o*-phenylenediamine (0.5 g) was dissolved in 10 mL ethanol and the solution was transferred to a poly(tetrafluoroethylene)-lined autoclaves. After heating at 180 °C in oven for 12 h and cooling down to room temperature naturally, red suspensions were obtained. The crude products were then purified with a silica column chromatography using mixtures of methylene chloride and ethanol as eluents. The process was repeated three times to remove excess impurities and unreacted precursors. After removing solvents and further drying under vacuum, the three purified R-CDs, G-CDs and B-CDs could be finally obtained in 10–20 wt% yields.

Results and discussion

The multicolor CDs were prepared *via* the solvothermal route based on the reaction of only *o*-phenylenediamine under different reaction conditions (Fig. 1). Although Jiang *et al.* reported RGB emitting CDs by carbonizing different substituted

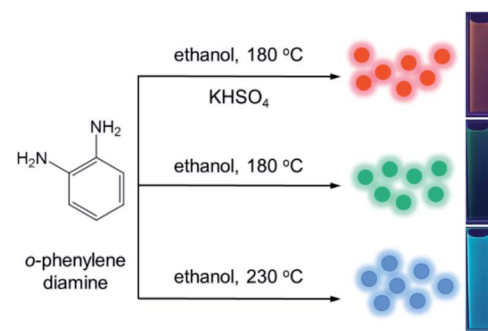


Fig. 1 Preparation of R-CD, G-CD, and B-CD tricolor CDs from *o*-phenylenediamine using different conditions. Photographs of tricolor dispersed in ethanol under $\lambda = 365$ nm UV irradiation.

phenylenediamine (*o*-, *m*-, *p*-) as precursors at 180 °C, we tried to find a catalyst that can activate phenylenediamine, to obtain different fluorescent color CDs more conveniently.¹⁴ We have tried to use strong acid such as hydrochloric acid as catalyst to active amino group for (*o*-, *m*-, *p*-) phenylenediamine. The *o*- and *m*-phenylenediamine showed red light-emitting after carbonization, but after adjusting the pH value to 7, the fluorescence color changed from red to green. After trying a lot of catalysts (such as copper sulfate, titanium isopropylate, pyrrolidine, potassium hydrogen sulfate), we found that *o*-phenylenediamine can be used to prepare CDs with stable red light-emitting at 180 °C under potassium hydrogen sulfate as the catalysis. In the optimization of concentration of precursors and temperature of carbonization, we found that blue fluorescent CDs could be obtained at higher concentration and reaction temperature without catalyst. At relatively low concentration, *o*-phenylenediamine can only produce green fluorescent CDs, which is consistent with the research of Jiang *et al.* The resulting CDs can be dispersed in various common organic solvents to obtain clear solutions, but they are insoluble in water. For example, clear RGB emitting solutions were formed when the CDs were dispersed in ethanol under UV irradiation ($\lambda_{\text{ex}} = 365$ nm; Fig. 1).

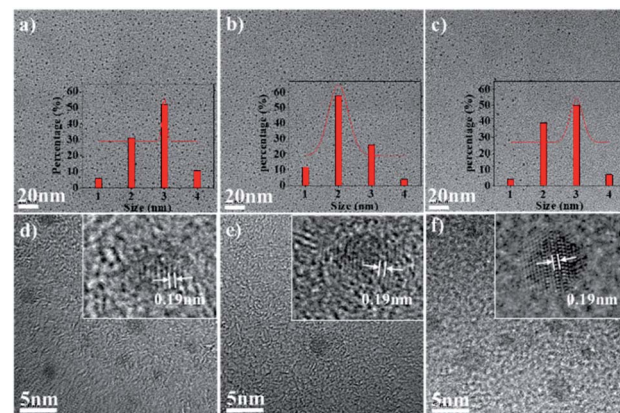


Fig. 2 (a–c) TEM images of R-CD, G-CD, and B-CD. Inset: histograms and Gauss fittings of particle size distribution and (d–f) enlarged TEM images of R-CD, G-CD, and B-CD.



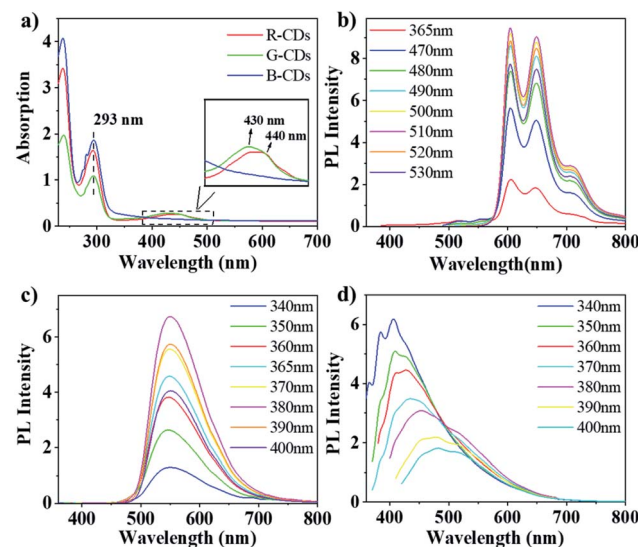


Fig. 3 (a) UV/Vis absorption spectra of R-CDs, G-CDs, and B-CDs ($c = 0.1 \text{ mg mL}^{-1}$); (b-d) PL emission spectra of R-CDs, G-CDs, and B-CDs in ethanol at different excitation wavelengths ($c = 0.1 \text{ mg mL}^{-1}$).

Transmission electron microscopy (TEM) was performed to examine the morphologies of the as-prepared samples. As shown in Fig. 2a-c, TEM images demonstrate that the R-CDs, G-CDs, and B-CDs were monodispersed and had similar sizes of *ca.* 2.5 nm. The high-resolution TEM images (Fig. 2d-f) of the samples show well-resolved lattice fringes of graphite carbon with an interplanar spacing of 0.19 nm.^{15,16} Obviously, the similar particle size of the three samples suggests that the quantum size effect was not the dominant mechanism responsible for the occurrence of chromatic emissions.¹⁷

The UV/Vis absorption spectra of the CDs were measured in ethanol, as shown in Fig. 3a. In the UV region, significant absorption peak is observed at 293 nm for three CDs, can be assigned to the intrinsic state ($n-\pi^*$) transition from the aromatic sp^2 domains (C=O and C=O).¹⁸ However, in the lower-energy region, three CDs show distinct absorption behavior. The absorption peak of 440 nm is shown for G-CDs, which is consistent with the literature.¹⁹ The absorption peak of R-CDs red-shift by 10 nm compared to that of G-CDs, which means that a longer conjugation system is formed. In contrast, B-CDs not show absorption in the lower-energy region, which indicate that there is no large conjugation structure.

Fig. 3b-d show the PL emission (PL) spectra of the three CDs recorded in ethanol solution, in which the emission maxima of R-CDs, G-CDs, and B-CDs can be observed at $\lambda = 600$, 541, and 406 nm, respectively. The emission spectra of B-CDs exhibit classical excitation-dependent properties, namely, red-shifting of the emission peaks with increasing excitation wavelength (Fig. 3d). According to previous reports, this shifting can be assigned to surface-defect emission.²⁰ According to previous reports, this shifting can be assigned to intrinsic and defect emission the spectra of B-CDs present an obvious blue-light emission under UV excitation (320–380 nm), with a peak at 406 nm and a PLQY of 10.0% under excitation at 340 nm. In contrast, the emission of G-CDs and R-CDs exhibit an

excitation-independent feature. For G-CDs (Fig. 3c), intense green emissions are observed, forming a wide emission band centered at 541 nm under excitations at 380–440 nm, and a PLQY of 10.5% was obtained at an excitation of 400 nm. Meanwhile, the R-CDs excited at 490–560 nm show two fluorescence peaks at 600 and 650 nm, as can be seen from the corresponding PL spectrum (Fig. 3b). A PLQY of 9.5% for the red-light emission was achieved under an excitation of 500 nm. The emission peak remained unchanged when changing the excitation wavelength, which differs from B-CDs emission, this can be attributed to nitrogen organic fluorophores, the so-called molecular states emission.^{20–22}

Fourier transform infrared (FT-IR) spectroscopies were conducted to characterize the surface functional groups of the samples. As shown in Fig. 4a, the three CDs exhibit similar FT-IR spectra, indicating their similar chemical compositions. R-CD, G-CD, and B-CD possess abundant hydrophilic groups according to the O-H and N-H stretching vibrations at 3050–3650 cm^{-1} , ensuring good solubility in polar organic solvents.^{16,23} Other peaks corresponding to the functional groups, such as C=O (1630 cm^{-1}), H-N (1500 cm^{-1}), C=C (1270 cm^{-1}), C-NH-C (1160 cm^{-1}), C-C (1030–1060 cm^{-1}), were also observed, which can be partially attributed to the stretching vibrations of the bonds between C, N, and O in the aliphatic group. Moreover, the origin of the distinct chromatic emissions was confirmed by determining the PL lifetimes (Fig. 4b). Average lifetimes of 3.6, 4.4, and 2.6 ns were obtained in ethanol for the red, green, and blue emissions. The corresponding error bars of these CDs are shown in Fig. S1.[†] The PL lifetime of B-CDs is much shorter than that of RG-CDs, indicating that they have different PL mechanisms between B-CDs and RG-CDs.²⁵

X-ray photoelectron spectroscopy (XPS) measurements were performed to gain more insight into the chemical bond

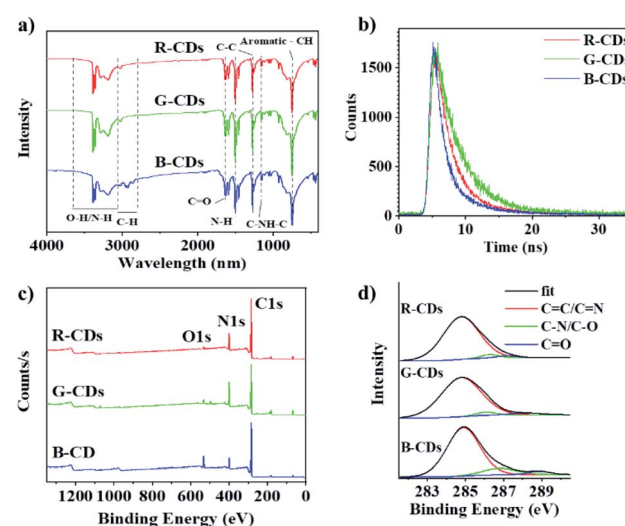


Fig. 4 (a) FT-IR spectra of R-CDs, G-CDs, and B-CDs. (b) Photoluminescence lifetime decay of R-CDs, G-CDs, and B-CDs in ethanol ($c = 0.1 \text{ mg mL}^{-1}$; $\lambda_{\text{ex}} = 500 \text{ nm}$ for R-CD; $\lambda_{\text{ex}} = 400 \text{ nm}$ for G-CD; $\lambda_{\text{ex}} = 340 \text{ nm}$ for B-CD). (c) XPS survey spectra of R-CDs, G-CDs, and B-CDs. (d) High-resolution C 1s spectra of different CDs.

Table 1 Elemental proportions and chemical bonds in RGB-CDs

	R-CD	G-CD	B-CD
C 1s	81.5%	75.2%	79.7%
O 1s	2.6%	2.9%	9.7%
N 1s	15.9%	21.9%	10.6%
C=C/C=N	93.0%	92.0%	85.0%
C-N/C-O	4.0%	4.0%	10.0%
C=O	3.0%	4.0%	5.0%

composition. As shown in Fig. 4c, the XPS survey spectra of different CD samples demonstrate three main peaks at 285.0, 399.0, and 532.0 eV, respectively, corresponding to C 1s, N 1s, and O 1s, indicating that all the CDs mainly comprise C, N, and O. Table 1 shows the proportions of the three elements in R-CD, G-CD, and B-CD. As can be seen, the element proportions differ appreciably between different samples with B-CD having the highest O 1s intensity, this may be attributed to the fact that B-CD are prepared at relatively higher carbonization temperatures. The high-resolution XPS spectra (Fig. 4d and Table 1) of C 1s confirm the existence of sp^2 C=C/C=N bonds (284.8 eV), C-N/C-O bonds (286.3 eV), and C=O bonds (288.2 eV). The proportion of the C=C/C=N components increased from B-CDs to G-CDs to R-CDs, which signify more sp^2 carbon structures are formed.

According to previous reports, the solvothermal route of phenylenediamine can form polyaniline fluorophore generally,²⁴ like as formation of G-CDs in this study. The addition of potassium hydrogen sulfate can activate the amino group and enhance the solvothermal reaction activity, which may form a phenylenediamine with larger conjugate domain than that of G-CDs, like as formation of R-CD. However, at higher reactant concentration and reaction temperature, phenylenediamine may not be able to slowly form a thermodynamically stable polyaniline, can only form a kinetically stable molecule, resulting in the lack of conjugated structure in the interiors of the CDs. In B-CDs, high degrees of oxidation leading to rich surface-defect density, electrons and holes radiatively recombine under illumination by excitation light, causing blue photoluminescence (Fig. 5a). The oxygen-containing functional group such as C-O, C=O, and O=C-OH in B-CDs surface produce many distinct energy levels, with the fluorescent emission then depending on excitation wavelength.^{25,26} Therefore, we speculate that the fluorescence of B-CDs originates from the surface-defect state, and the fluorescence of R- and G-CDs originate the molecular state.

In order to explore the stability of the fluorescence of CDs, we studied its spectral changes in different visible and ultraviolet light continuous irradiation time (Fig. S2†), different temperatures (Fig. S3†) and different polar solvent environment (Fig. S4†). The maximum attenuation rate of the fluorescence intensity of the CDs under visible light for 7 days is less than 15%. Meanwhile, the attenuation rate of the fluorescence intensity of the CDs is less than 20% after 8 hours of continuous ultraviolet light ($\lambda = 365$ nm) (Fig. S5a and b†). When the temperature of the CDs reaches 80 °C the fluorescence attenuation rate of the CDs also has not more than 20% (Fig. S5c†).

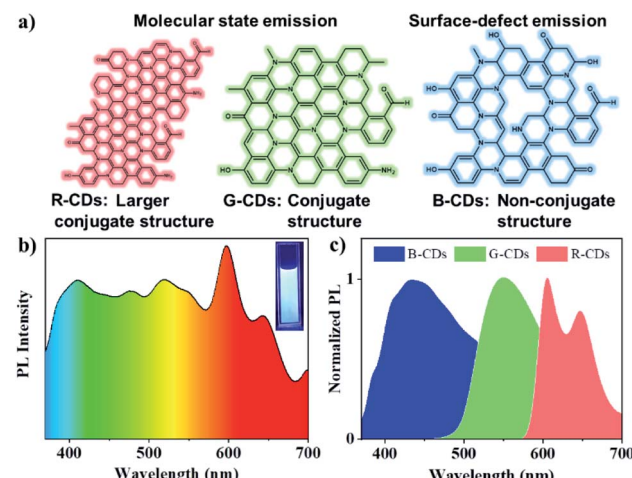


Fig. 5 (a) A possible PL emission mechanism for RGB-CDs. (b) White PL spectrum of the RGB-CD solution at 365 nm excitation. The insets show photographs of the RGB-CDs solution under 365 nm UV irradiation. (c) Normalized PL spectra of the RGB-CDs at 365 nm excitation.

The CDs show some stability in different polar solvents, especially B-CDs, whose emission peak ranges within 10 nm, and the fluorescence ranges of G-CDs and R-CDs are 30 nm and 50 nm. The results show that RGB-CDs have good stability which makes them have great potential for sustainable applications in lighting equipment.

One application of RGB-CDs is to achieve white glow. Considering the liquid fluorescence stability of CDs, we prepared 1 mg mL⁻¹ solutions of the tricolored CDs, and a stable white fluorescent CDs solution was obtained by mixing the solutions in a R-CDs : G-CDs : B-CDs ratio of 1 : 1 : 2 (Fig. 5b). Under UV light of 365 nm, their emission maxima locate at 415, 550, and 605 nm, respectively, almost the same with those of the original CDs (Fig. 5c). The 1931 CIE chromaticity coordinate of the white fluorescent CDs was (0.38, 0.37) (Fig. S6†).

Conclusions

In summary, we developed a simple method to synthesize red, green, and blue luminescent CDs *via* the solvothermal method by changing the reaction conditions. The three CDs showed bright RGB luminescence in a solution. Under the optimal excitation wavelength, the fluorescence QY of R-CDs, G-CDs, and B-CDs reached 9.5%, 10.5%, and 10.0%, respectively. The different PL emissions of RGB-CDs can be attributed to the differences in the conjugate structure and surface state. This study provides a new method for the preparation of RGB-emitting CDs and a new way of thinking for developing low-cost, environmentally friendly, and high-performance white LEDs.

Author contributions

Conceptualization, Y. A. and C. L.; methodology, Y. A. and X. L.; writing—original draft preparation, Y. A.; writing—review and



editing, K. X., X. C., Y. L., and Y. Z.; visualization, X. L.; supervision, C. W.; project administration, Y. Z.; funding acquisition, C. L. All authors have read and agreed to the published version of the manuscript.

Conflicts of interest

The authors declare that the research was conducted in the absence of any commercial or financial relationships that could be construed as a potential conflict of interest. There are no conflicts to declare.

Acknowledgements

This work was partially supported by the National Natural Science Foundation (No. 21961036, 31660179, and 31960297). The study also was supported by the project of Yunnan Province (No. 202101AT070041 and 202002AA10007) and Key Laboratory for Forest Resources Conservation and Utilization in the Southwest Mountains of China No. KLESWFU-201908.

Notes and references

- 1 S. Diao, X. Zhang, Z. Shao, K. Ding, J. Jie and X. Zhang, *Nano Energy*, 2017, **31**, 359–366.
- 2 F. Guo, X. Huang, Z. Chen, H. Sun and W. Shi, *Sep. Purif. Technol.*, 2020, **253**, 117518.
- 3 Z. Zhang, Y. Lei, X. Yang, N. Shi, L. Geng, S. Wang, J. Zhang and S. Shi, *J. Mater. Chem. B*, 2019, **7**, 2130–2137.
- 4 J. Xu, Y. Miao, J. Zheng, H. Wang, Y. Yang and X. Liu, *Nanoscale*, 2018, **10**, 11211–11221.
- 5 H. Wang, C. Sun, X. Chen, Y. Zhang, V. L. Colvin, Q. Rice, J. Seo, S. Feng, S. Wang and W. Y. William, *Nanoscale*, 2017, **9**, 1909–1915.
- 6 J. R. Adsetts, R. Zhang, L. Yang, K. Chu, J. M. Wong, D. A. Love and Z. Ding, *Front. Chem.*, 2020, **8**, 580022.
- 7 J. Zhu, X. Bai, J. Bai, G. Pan, Y. Zhu, Y. Zhai, H. Shao, X. Chen, B. Dong and H. Zhang, *Nanotechnology*, 2018, **29**, 085705.
- 8 T. Zhang, F. Zhao, L. Li, B. Qi, D. Zhu, J. Lu and C. Lü, *ACS Appl. Mater. Interfaces*, 2018, **10**, 19796–19805.
- 9 C. Sun, Y. Zhang, Y. Wang, W. Liu, S. Kalytchuk, S. V. Kershaw, T. Zhang, X. Zhang, J. Zhao, W. W. Yu and A. L. Rogach, *Appl. Phys. Lett.*, 2014, **104**, 261106.
- 10 Y. F. Yuan, Z. Wang, X. Li, Y. Li, Z. A. Tan, L. Fan and S. Yang, *Adv. Mater.*, 2017, **29**, 1604436.
- 11 K. Jiang, S. Sun, L. Zhang, Y. Lu, A. Wu, C. Cai and H. Lin, *Angew. Chem.*, 2015, **127**, 5450–5453.
- 12 J. Zhu, X. Bai, X. Chen, Z. Xie, Y. Zhu, G. Pan, Y. Zhai, H. Zhang, B. Dong and H. Song, *Dalton Trans.*, 2018, **47**, 3811–3818.
- 13 K. Zhao, X. Zheng, H. Zhang, M. Xu, S. Wang, Q. Yang and C. Xiong, *J. Alloys Compd.*, 2019, **793**, 613–619.
- 14 T. Guo, B. H. Yuan and W. J. Liu, *Org. Biomol. Chem.*, 2018, **16**, 57–61.
- 15 X. Chen, X. Bai, C. Sun, L. Su, Y. Wang, Y. Zhang and W. Y. William, *RSC Adv.*, 2016, **6**, 96798–96802.
- 16 S. Qu, D. Zhou, D. Li, W. Ji, P. Jing, D. Han, L. Liu, H. Zeng and D. Shen, *Adv. Mater.*, 2016, **28**, 3516–3521.
- 17 H. Ding, S. B. Yu, J. S. Wei and H. M. Xiong, *ACS Nano*, 2016, **10**, 484–491.
- 18 X. Wang, Y. Feng, P. Dong and J. Huang, *Front. Chem.*, 2019, **7**, 671.
- 19 X. T. Zheng, A. Ananthanarayanan, K. Q. Luo and P. Chen, *Small*, 2015, **11**, 1620–1636.
- 20 T. Zhang, J. Zhu, Y. Zhai, H. Wang, X. Bai, B. Dong, B. Dong, H. Wang and H. Song, *Nanoscale*, 2017, **9**, 13042–13051.
- 21 S. Zhu, Y. Song, X. Zhao, J. Shao, J. Zhang and B. Yang, *Nano Res.*, 2015, **8**, 355–381.
- 22 J. Schneider, C. J. Reckmeier, Y. Xiong, M. von Seckendorff, A. S. Susha, P. Kasák and A. L. Rogach, *J. Phys. Chem. C*, 2017, **121**, 2014–2022.
- 23 Y. Zhai, X. Bai, H. Cui, J. Zhu, W. Liu, T. Zhang, B. Dong, G. Pan, L. Xu and S. Zhang, *Nanotechnology*, 2017, **29**, 025706.
- 24 C. Tan, X. Su, C. Zhou, B. Wang, Q. Zhan and S. He, *RSC Adv.*, 2017, **7**, 40952–40956.
- 25 L. Ai, Y. Yang, B. Wang, J. Chang, Z. Tang, B. Yang and S. Lu, *Sci. Bull.*, 2021, **66**, 839–856.
- 26 J. Douda, C. R. González-Vargas, I. I. Mota-Díaz, E. V. Basiuk, X. A. Hernández-Contreras, J. A. Fuentes-García, J. Bornacelli and C. Torres-Torres, *Nano Express*, 2020, **1**, 030009.

